Study of the role of dendrites in the orientation tuning of a single L2/3 pyramidal neuron model

By

GEORGIA KONTODIMOU

Faculty of Medicine
UNIVERSITY OF CRETE

A dissertation submitted to the University of Crete for the partial fulfillment of the requirements of the graduate program "NEUROSCIENCE" in the Faculty of Medicine.

SEPTEMBER 2016

Abstract

Orientation tuning, i.e. the preferential response to stimuli with a particular orientation, is a fundamental feature selection process occurring in V1. Although it has been more than half a century that Hubel and Wiesel conducted their pioneering studies on the visual system, the dendritic basis of orientation preference has just started to be deciphered. In addition, the morphology of the pyramidal neuron with its apical and basal trees lying in different layers of the cortex and thus receiving inputs of distinct nature, could endow with specific and distinct roles in sensory processing.

In this study we investigate the role of basal and apical trees, as well as the role of dendritic spikes in orientation tuning at the single cell level by implementing a biophysically and morphologically detailed reconstruction of a layer 2/3 V1 mouse neuron using the NEURON simulation environment. To assess the possible contribution of biophysical mechanisms we simulate the blockade of voltage-gated Na^+ channels and/or NMDARs in basal andapical dendrites and we perform both somatic and dendritic recordings.

Our results show that orientation tuning of the neuron seems to follow the tuning of the basal tree. In addition, blockade of both the NMDARs and the voltage-gated Na^+ channels, under increase in AMPA conductance, showed that the basal tree has a more significant role in shaping orientation selectivity in layer 2/3 V1 pyramidal neurons. Regarding dendritic spikes, we observed Na^+ spikes and we found that they are significantly less in the orthogonal orientation. We failed to observe NMDA spikes, but this needs to be further analyzed.

In conclusion, our study helps to dissect the contributions of two key ionic conductances found in the dendrites of layer 2/3 V1 mouse neurons. Moreover, we suggest a dominant role of the basal rather than the apical tree in fine tuning the orientation preference of these cells.

Dedicated to my dad.

ACKNOWLEDGEMENTS

First of all, I would like to thank dr. Panayiota Poirazi for giving me the opportunity to become a member of the computational biology lab and for her guidance during my master thesis. I am also very grateful to my post doc supervisor, Nassi Papoutsi, for both her scientific and personal support through these months. Also, I would like to thank prof. Kiki Thermou and Kiriaki Sidiropoulou for being in my thesis' comittee. Of course, many thanks go to my lab-mates (Alexandra, Pavlos, Spiros, Eleni, Panagiotis P., Panagiotis B., Stefanos, George) for sharing our everyday laughs and worries. Lastly, I thank my firends and family. Of course, my most grateful thanks go to Manolis for his extreme patience and constant encouragement throughout the duration of the master program.

TABLE OF CONTENTS

List of Tables

List of Figures

Figure **Page**

CHAPTER 1

INTRODUCTION

Living organisms are continuously flooded with environmental stimuli of variant modalities: visual, auditory, olfactory, tactile, gustatory. After these stimuli are transduced, they are relayed by the thalamus to the proper sensory cortex in order to be further processed, combined and conceptualized, helping us to perceive the world. This cortical process has been found to occur in a circuit level, single neuronal level and the past few years methodological developments have revealed that it also occurs in the dendritic level. However, we are far from having the complete picture, a picture that could possibly involve a set of elegant common principles that underlie the processing of all our senses. This question is of fundamental importance and current experimental and theoretical neuroscience research using top-notch technology is aiming to address it.

1.1 Sensory processing

Photons, mechanical and chemical stimuli are received by the appropriate sensory organ and are "translated" to the language of the brain: electrochemical signals. This process is called transduction and is the first step of sensory processing. Then, for most of the senses, the information travels to the thalamus, the brain's relay center, and from there goes hierarchically from primary sensory cortices to secondary and higher order association cortices. During this course, the information from the external world becomes realized, combined with information from other modalities, conceptualized,combined

with our past experiences and our internal representation of the world (Larkum, 2012) and leads to a behavioural outcome (Hudspeth and Logothetis, 2000).
One fundamental property of cortical sensory processing is stimulus selectivity. Certain neurons in sensory cortices exhibit a higher activity in response to specific stimuli: neurons in V1 show orientation and direction selectivity (Hubel & Wiesel, 1959), in primary auditory cortex there are neurons that respond better to specific tone frequencies (Goldstein et al., 1970), neurons in the olfactory cortex show selectivity to specific combinations of odorants (Yoshida & Mori, 2007) and in the barrel cortex certain neurons are more responsive to certain whisker angular deflections (Lichtenstain et al., 1990). Although this property of sensory neurons has been studied a lot during the several past decades, especially in the visual system, the question of its emergence and function still remains open.

1.2 Orientation selectivity in the mouse visual system

1.2.1 why use the mouse?

The first (Hubel & Wiesel, 1959, 1968) and most of the following studies of feature selectivity, especially for the visual system, were conducted in carnivores and primates. The most important reason the progress in the particular field has been slowed down are the technical limitations. To study cortical sensory processing one has to record the sensory responses of the animal, which has to be in vivo, and image the neuronal connectivity underlying this particular response, which up until recently could only be done in vitro.
The technological developments in genetics, during the past decade, that allow manipulation in the single-cell level (Luo et al. 2008 for a review) and the new advances in calcium imaging and optogenetics (Arenkiel et al. 2007) have made mouse a prominent animal model for the study of the mammalian sensory processing. The study of Niell & Stryker in 2008 of the properties of the mouse visual cortex confirmed that, despite discrepancies among the species, the fundamental properties of sensory processing are conserved in the mouse and its study could give important insights of the big picture.

1.2.2 The visual pathway

Photons enter the brain through the eyes where light is transformed to electrical signals by the photoreceptors in the retina. Mouse's retina is full of cones, helping them to see under low-light conditions. The electrical signals, through the axons of the retinal ganglion cells, arrive at the optic chiasm where over 90% of the axons cross the midline, in contrast to the almost 50% in higher species. This is due to the lateral position of the eyes in the mouse resulting to 50% binocularity in mouse and 135% in man (Drager 1978). The next stop of the path is the lateral geniculate nucleus of the thalamus (LGN). The mouse LGN is not laminar, in contrast to the primate LGN which has eye-specific laminae. From LGN thalamocortical axons project to (mainly) the layer IV neurons of the primary visual cortex (V1). A schematic representation can be seen in fig. 1.1.

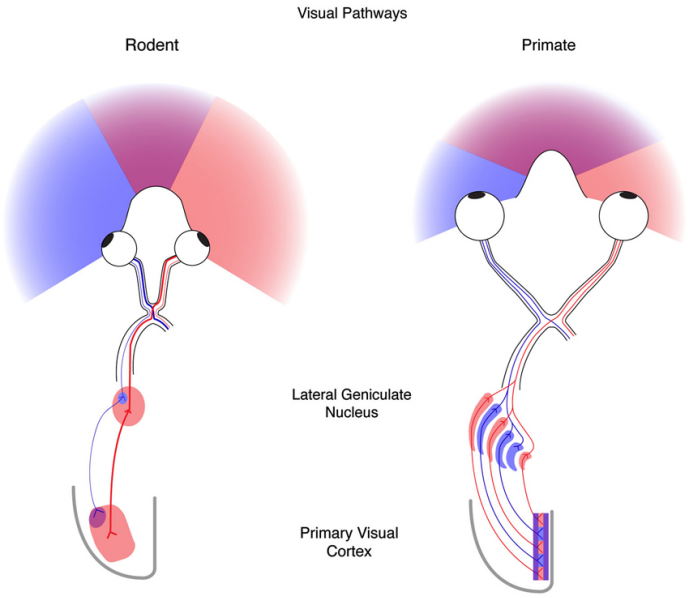

FIGURE 1.1. the visual pathway of rodents and primates. Figure reproduced from (Hubener 2003).

1.2.3 Orientation selectivity

It has been more than half a century that Hubel and Wiesel conducted their pioneering studies on the visual system of the cat (Hubel & Wiesel 1959) and later on the visual system of primates (Hubel & Wiesel 1968). Recording the activity of V1 neurons they demonstrated that a large population of these neurons respond vigorously to edges of a particular orientation and weakly, or not even at all, at the orientation with a difference

of 90^o (fig. 1.2). The orientation that causes the vigorous response is the preferred orientation of the neuron, whereas the orientation with the weakest response is the orthogonal one. Although the visual system of the mouse has lower resolution, it has been shown that it has a level of orientation selectivity similar to that of species with more developed system (Neill & Stryker 2008).

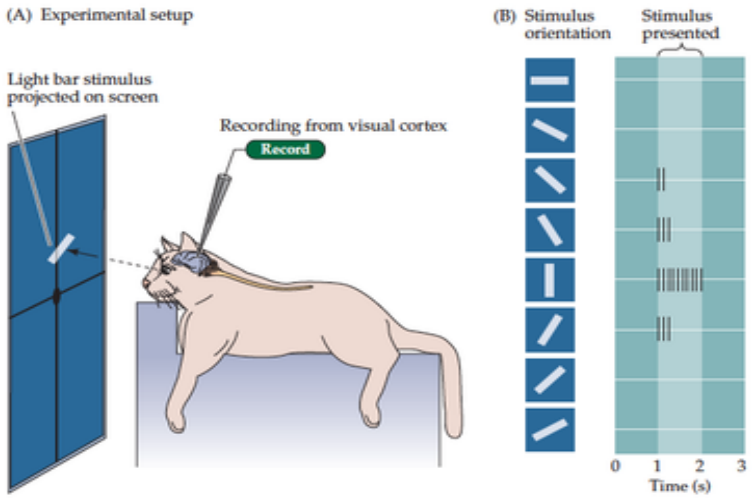

FIGURE 1.2. Hubel and Wiesel recorded from neurons in the visual cortex of the cat to find out that certain neurons were more responsive to lighting bars of a particular orientation and no responsive to the perpendicular one. Figure reproduced from Purves, Neuroscience, 3rd edition.

1.2.4 Emergence of orientation selectivity

Hubel and Wiesel proposed a simple model of excitatory convergence for the emergence of orientation. In their feedforward model untuned inputs from LGN neurons with aligned receptive fields along an axis converge to a layer 4 neuron in V1. (fig. 1.3)

Although this elegant model has stood for several decades and is still used and is consistent with several studies, recent findings have begun to challenge it. In 2013 two separate studies (Lien et al. 2013, Li et al. 2013) using optogenetic techniques isolated the thalamocortical element and found that it is indeed orientationally tuned, but it accounts for only the one third of the total excitation in layer 4 neurons. This thalamic component is similarly tuned with the layer 4 neurons which amplify this component. In addition to the layer 4 input it has been found that there is a di-synaptic circuit which links the retina with the superficial V1 cortical layers (Cruz-Martin 2014).

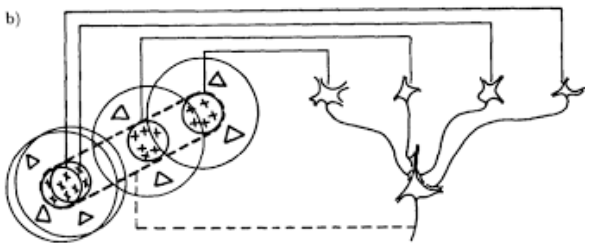

FIGURE 1.3. Hubel and Wiesel's feedforward model. Figure reproduced from (Hubel and Wiesel 1962).

1.2.5 V1 architecture and connectivity

Primary visual cortex (V1) in many mammalian species, such as primates, cats and ferrets, has an exquisitely organized functional architecture. Hubel and Wiesel in their experiments found that neuronal preferences varied systematically as the electrode was moving across the cortical surface, creating a columnar orientational architecture. Rodents, however, seem to lack an architecture and their V1 is organized in a salt-and-pepper fashion (Ohki et al., 2005) (fig. 1.4)

Even in the absence of columnar architecture, there is a functionally biased connec-

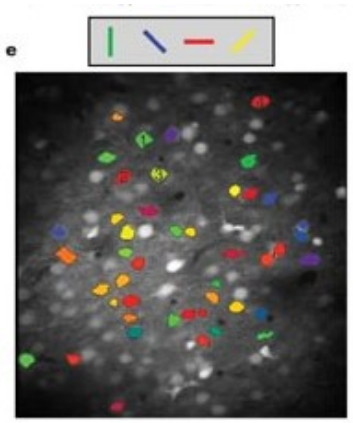

FIGURE 1.4. Rat orientation map. Figure reproduced from (Ohki 2005).

tivity. Neurons having similar orientation preference are more likely to connect with each other comparing with those having large difference in orientation preference and these connections are mostly bidirectional (Ko et al. 2011). It is worth mentioning that functionally organized connectivity is not required for the neurons to be orientationally tuned, as mice at eye-opening already have orientation selectivity. Instead this connectivity increases the robustness and reliability of the neuron's response (Ko et al.

2013). Although the strong connected pairs are very few compared to the weak ones, they account for the majority of the total synaptic weight and directly contribute to the neuron's feature selectivity (Cossell et al. 2015).

Regarding inhibition in V1, studies have shown that inhibitory interneurons receive many inputs from neighbouring pyramidal neurons of different orientation tunings which cause them to be quite broadly tuned. (Bock et al. 2011, Hofer et al. 2011). Even though broadly tuned, inhibitory interneurons sharpen the already existing orientation selectivity by lowering the membrane potential for all orientations, but mostly for the orthogonal orientation (Liu et al. 2011).

1.3 The role of dendrites

1.3.1 Regenerative events

For a long time dendrites were thought to play a passive role in synaptic input integration and they were considered to be passive transporters of these inputs to the soma of the neuron, where the actual integration takes place. Theoretical studies (Rall 1964, Koch 1982) began to question this assumption and experimental work proved them right. It is now known that dendrites posses the passive and active (i.e. voltage-dependent channels) (Jaffe 1992) machinery to support nonlinear integration of the synaptic inputs and so increase the computational capacity of a neuron (Poirazi & Mel, 1999).

Specifically, it is now known that in some neurons action potentials can propagate back to the dendritic tree (back-propagating action potentials or bAPs), depending on the structure of the dendritic tree, the distance from the soma and the availability in Nav and Kv channels (Stuart et al. 1997, Vetter et al. 2001, Colbert et al. 1997).

Another property of some neurons that has been revealed the past few years is that they can produce threshold-based, regenerative electrogenic activity, referred to as dendritic spikes. These events are often locally produced and don’t make it to the soma, but they do affect the firing of the neuron by increasing the propability of the generation of an action potential in the soma and can interact with bAPs. There are three different types of dendritic spikes that are generated by different mechanisms and supported by different types of channels, namely calcium spikes, sodium spikes and NMDA spikes. Each of them has distinct characteristics as seen in figure 1.5 and it has been shown

that L2/3 neurons do support dendritic spikes (Larkum 2007).

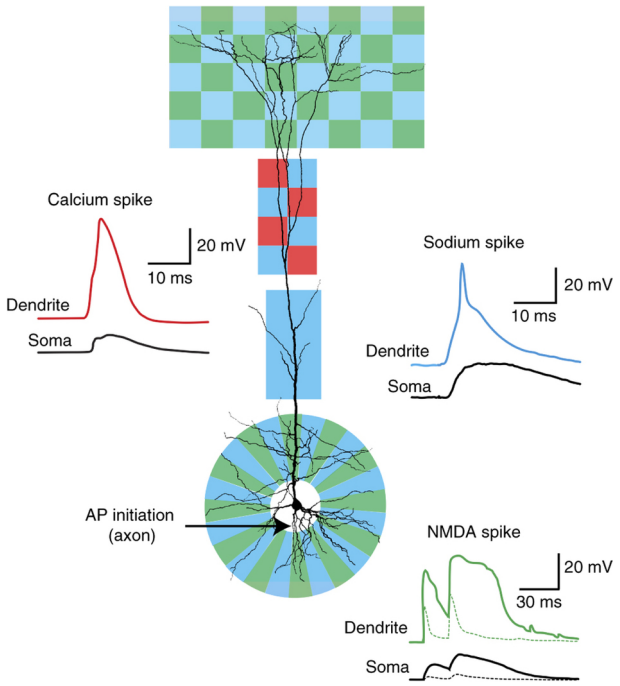

FIGURE 1.5. Dendritic spikes. Figure reproduced from (Stuart & Spruston 2015).

1.3.2 Effect on feature selectivity

Recent studies in the mouse have shown the active involvement of dendrites in stimulus selectivity and across the layers of sensory cortices there have discovered all kinds of integration modes: linear, supralinear and sublinear. Jia et al. in 2010 combined whole-cell recordings with two-photon calcium imaging in vivo to find out that dendritic hotspots of similar orientation preferences that act as entry inputs for sensory features are not clustered, instead they are widely dispersed over various dendrites. In addition, they found out that even though somatic selectivity is cancelled by hyperpolarization, the dendritic selectivity is not. These findings were confirmed in 2013 by Chen et al., who in addition observed that the average of the orientation preference of the spines is similar to that of the parent neuron.

Sensory-evoked dendritic spikes, or calcium transients that could be dendritic spikes, have been observed in neurons of various sensory cortices of the mouse. In the visual cortex, where they are thought to enhance orientation selectivity (Smith et al.

2013), in the auditory cortex (Chen et al. 2011), in the somatosensory cortex (Palmer et al. 2014) and in the barrel cortex (Lavzin et al. 2012). On the other hand, there has also been observed sublinear integration underlying binocular processing of orientation selectivity (Longordo et al. 2013, Zhao et al. 2013). Lastly, a recent computational study by Caze (Caze et al. 2015) showed that nonlinear dendrites make a neuron's response to sensory stimuli more robust.

1.3.3 Pyramidal morphology effect

Pyramidal neurons have two morphologically distinct dendritic components: the basal dendrites and the apical tree. These two have different synaptic input profiles. Basal dendrites receive mainly feed-forward, external sensory input, whereas the apical tree that extends to layer 1 receives intracortical feedback inputs. Although apical tuft dendrites are far from the soma and therefore cannot influence its firing, events like bAPs and/or dendritic spikes can play a key role in linking the activity of basal and apical dendrites. This property has made the pyramidal neuron an attractive candidate to be the cellular associative element that couples feed-forward, sensory information with feedback information of the internal representation of the world, as seen in figure 1.6 (Larkum 2013).

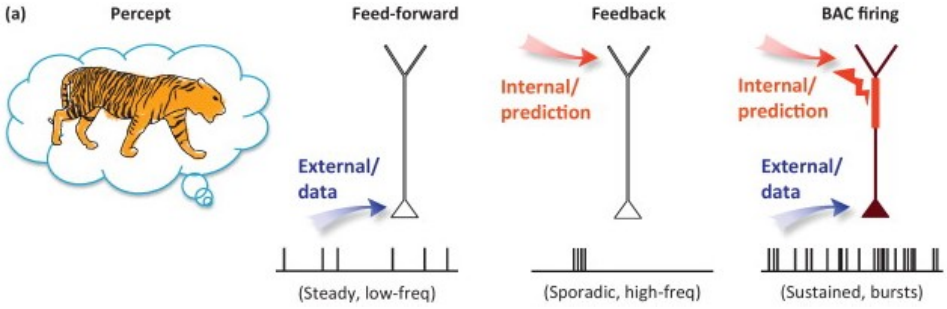

FIGURE 1.6. The pyramidal neuron as coupler of feed-forward and feedback information. Figure reproduced from (Larkum 2013).

1.4 Motivation of the study

From the previous, it is evident that the role of dendrites in sensory processing and in particular in feature selectivity has only recently begun to be deciphered. More specifically, there is still a lot of information missing regarding orientation selectivity

and how basal and apical trees interact to produce this feature. Furthermore, the role, if any, of dendritic spikes in this process remains unknown. Therefore, in this study we aim to investigate the role of basal and apical trees and the involvement of dendritic NA^+ and NMDA spikes in orientation tuning at the single cell level.

CHAPTER 2

MATERIALS & METHODS

2.1 Hardware & Software

All single cell and network simulations were implemented in the NEURON simulator package (Carnevale Hines 2006), version 7.3. Simulations exploring multiple parameters were processed by a cluster consisting of 312 High Performance CPU cores and 1.150 Gigabytes of RAM, running Red Hat -Centos Linux (version 6.5) and administered by the Computational Biology Lab (CBL) of the Institute of Molecular Biology and Biotechnology (IMBB) of the Foundation for Research and Technology Hellas (FORTH). Single testing trials were run on a dedicated 28-core, 128 GB RAM Linux Server. Data analysis was conducted with MATLAB (Mathworks Inc.).

2.2 The Model

2.2.1 Morphology

A biophysically and morphologically detailed reconstruction, provided by the Smirnakis lab (Baylor College of Medicine, Houston), of a layer 2/3 V1 mouse neuron was implemented using the NEURON simulation environment (Papoutsi 2016). The model consists of the following compartments: the soma, the axon, 7 basal compartments and 42 apical. The lengths and diameteres of the compartments are shown in table 2.1.

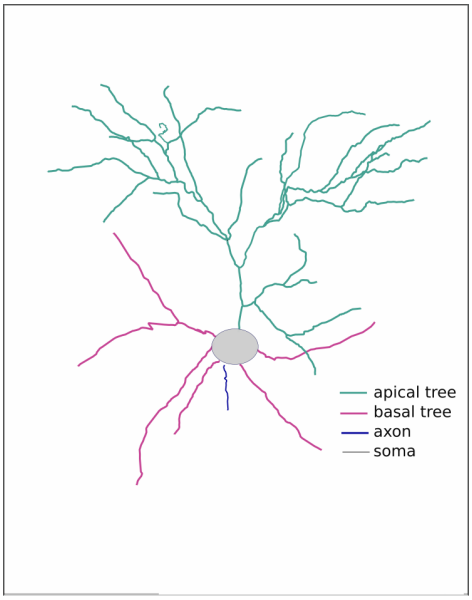

FIGURE 2.1. Morphology of the L2/3 pyramidal model neuron.

apical	diameter	length	apical(cont'd)	diameter	length	basal	diameter	length
1	2.0216273	26.713217	22	1.5347144	53.757513	1	0.57281887	155.31885
2	2.0599999	35.602371	23	1.0584665	34.91004	2	1.0377938	96.981879
3	2.0599999	26.854963	24	0.88	54.355926	3	0.77418113	134.2232
4	1.6953169	46.438015	25	0.66000003	94.311948	4	1.3508789	68.550425
5	1.4400345	35.974074	26	0.64042471	64.178843	5	0.74343258	114.19072
6	0.94999999	18.583492	27	0.49612789	24.833051	6	0.77999277	101.50537
7	0.94999999	8.0185342	28	0.37315069	25.3392	7	0.97363327	120.20713
8	0.72234623	99.551035	29	0.74728925	99.800487			
9	0.50999999	60.599094	30	0.67297454	30.031706			
10	0.66000003	120.47102	31	0.66000003	66.618526			
11	0.73000002	30.633428	32	0.66000003	37.685607			
12	0.73000002	16.60665	33	0.55860212	81.576269			
13	0.73000002	49.444612	34	0.58999997	109.91676			
14	0.58999997	77.123261	35	0.70935009	103.44139			
15	0.50999999	13.026379	36	0.50999999	154.69298			
16	0.39438973	85.740457	37	0.73000002	14.074175			
17	0.44	68.607614	38	0.7106648	34.875504			
18	0.74756876	118.82558	39	0.44146318	62.743879			
19	0.73000002	4.5128419	40	0.44	38.272968			
20	0.67128373	103.76853	41	0.58999997	46.799915			
21	0.58999997	92.41145	42	0.55938123	80.396545			

Table 2.1: Length and diameter of each compartment

2.2.2 Passive properties

The passive properties of the model neuron are:

* membrane capacitance (C_m)1.2μF cm^{-}2
* membrane resistance (Rm) 11000 Ω cm^2
* axial resistance (Ra) 100 Ω cm
* resting membrane potential was set at -79mV
* input resistance (R_{in}) was 129 MΩ (Cho et al., 2008, 2010; Smith et al., 2013)
* membrane time constant was 17 ms (Cho et al., 2010)

In the basal and apical dendrites, C_m was doubled to account for dendritic spines.

2.2.3 Active properties

The model includes the following active mechanisms (Smith et al., 2013):

* fast voltage-dependent Na channels.
* delayed rectifier K channels.
* slow voltage-dependent K channels.
* A-type K channels.
* Ca -activated K channels.
* high & low voltage-activated Ca2+ channels.

2.2.4 Synaptic mechanisms

Synaptic mechanisms included:

* AMPA
* NMDA
* GABA$_a$

conductance (mS/cm^2)	soma	apical	basal
g_{na}	0.050	0.303	0.303
g_{Kdr}	0.05	1.5*10^{-3}	1.5*10^{-3}
g_{Km}	2.8*10^{-3}	1.27*10^{-3}	1.27*10^{-3}
g_A	5.4	diameter<=0.8μm: 108 diameter<=0.8μm: 10.8	diameter<=0.8μm: 108 diameter<=0.8μm: 10.8
g_T	0.03	x<=260μm: 0.029*sin(0.009*x+0.88) x>260μm: 0.012	0.03+6*10-5*x
g_{HVA}	0.05*10-3	x<=260μm: 0.049*sin(0.009*x+0.88) x>260μm: 0.02*10^{-}3	0.05*10-3+10-7*x
g_{Ca}	2.1*10-3	2.1*10-3	2.1*10-3

Table 2.2: Active conductances of the model

	conductance (nS)	$\tau_1(ms)$	$\tau_2(ms)$
NMDA	1.15	2	30
AMPA	0.84	0.1	2.5
GABA$_A$	1.25	0.2	1.4

Table 2.3: Synaptic parameters

Maximum synaptic density of 2 excitatory synapses (spines)/μm was assumed (DeFelipe and Farinas, 1992; Schuz and Palm, 1989). Excitatory synapses consisted of both AMPA and NMDA conductances. The total dendritic length of the model neuron is 3298μm and thus the total number of excitatory synapses was 6596. Distribution of synapses to individual dendritic compartments was adjusted so that dendrites have the same synaptic density, that is, each dendrite received number of synapses proportional to its length. Inhibitory synapses were set to 15% of the total number of synapses (Binzegger et al., 2004; DeFelipe and Farinas, 1992).

The distribution of the synapses was as follows:

* 60% of the excitatory synapses were randomly distributed in basal tree
* 40% of the excitatory synapses were randomly distributed in apical tree (DeFelipe and Farinas, 1992)
* 7% of the inhibitory synapses were located at the soma
* 60% of the inhibitory synapses were located at the basal tree

* 33% of the inhibitory synapses were located at the apical tree (DeFelipe et al., 2003)

2.3 Stimulation protocol

25% of the total number of excitatory synapses were stimulus-driven (Chen et al., 2013) and were randomly dispersed along the basal and apical trees (Jia et al., 2010). The rest 75% of excitatory synapses as well as the inhibitory synapses were independently driven by Poisson spike trains with mean frequency 0.1Hz.
The stimulus, which was presented with a delay of 500ms and lasted for 2 seconds and would vary from 0^o to 180^o with a step of 10^o, was simulated by Poisson spike trains with a frequency depending on the difference between the preferred orientation of the synapse and the presented orientation. The frequency of the stimulus was set to be 0.5Hz in order to produce a somatic firing frequency of 2-3Hz, in agreement with the existing experimental values.
The distribution of preferred orientations to synapses was based on (Chen et al., 2013). In particular, the distribution followed the sum of two Gaussians with $\sigma = 30^o$ centered on the orientation preference of the apical and basal dendritic tree.

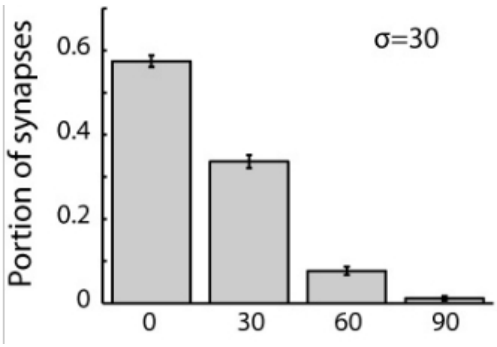

FIGURE 2.2. Portion of synapses in relation to the angular difference from the preferred orientation for a neuron with a preferred orientation of 0^o.

Orientation tuning in the model was assessed using the OSI metric, defined as:

$$OSI = \frac{R_{pref} - R_{ortho}}{R_{pref} + R_{ortho}} \tag{2.1}$$

The orientation tuning width (width at the half-maximum of the tuning curve) was calculated after fitting a double Gaussian to the tuning curve.

CHAPTER 3

RESULTS

3.1 Validation of the model

To validate the model a current step pulse of 0.16nA was given and the trace was compared to an experimental trace adapted from (Rhie et al., 2003).

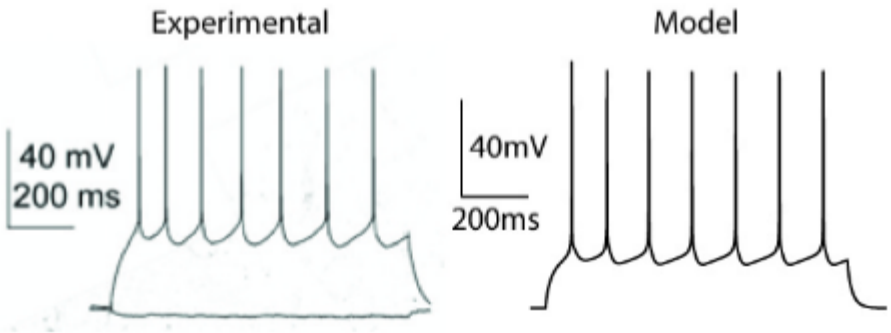

FIGURE 3.1. Experimental and model trace comparison.

The active and passive properties of the model were validated by comparing them to bibliography (Cho et al. 2010) and the results are shown in table 3.1.

	model	Cho et al. 2010
Vrest(mV)	-79	-78.56 ±1.34
IR (MΩ)*	123.475	125.2 ±8.2
τ (ms)	17.5	16 ±0.7
AP amplitude (mV)**	66.0556	67.8 ±1.8
AP threshold (mV)**	-41.8039	-37.7 ±1.3
AHP (mV)**	17.9117	13.3 ±0.5
P-T time(ms)**	38.6	55.3 ±2.7
AP adaptation**	1.1614	1.18 ±0.02

Table 3.1: Validation of active and passive properties

(*calculated with a hyperpolarizing current injection 0.04nA) (**calculated with a depolarizing current injection 0.16nA)

3.2 Reproduction of orientation selectivity

The simulation set up replicates orientation tuning in L2/3 neurons in the visual cortex, as seen in the tuning curve and the indicative traces for different orientations (0^o, 30^o , 60^o , 90^o) in figure 3.2.

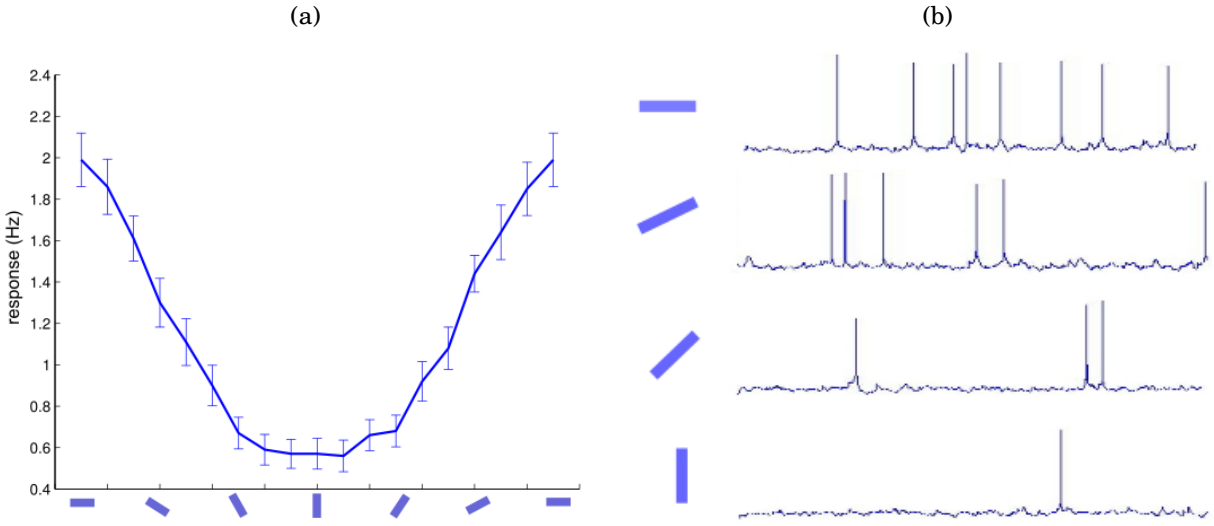

FIGURE 3.2. (a) Tuning curve for a preferred orientation of 0^o degrees. (b) Exemplar traces of different orientations for a preferred orientation of 0^o degrees.

3.3 Apical vs basal dominance

To see if there is a different contribution of the basal versus the apical tree in the orientation tuning of the neuron, we kept the apical tree tuned to 0^o and varied the tuning of the basal tree from 0^o to 90^o with a step of 10^o and examined the tuning of the whole neuron, i.e. the somatic responses. Orientation tuning of the neuron seems to follow the orientation tuning of the basal tree. Yet, there is a limit in the difference that supports optimal properties in orientation tuning.

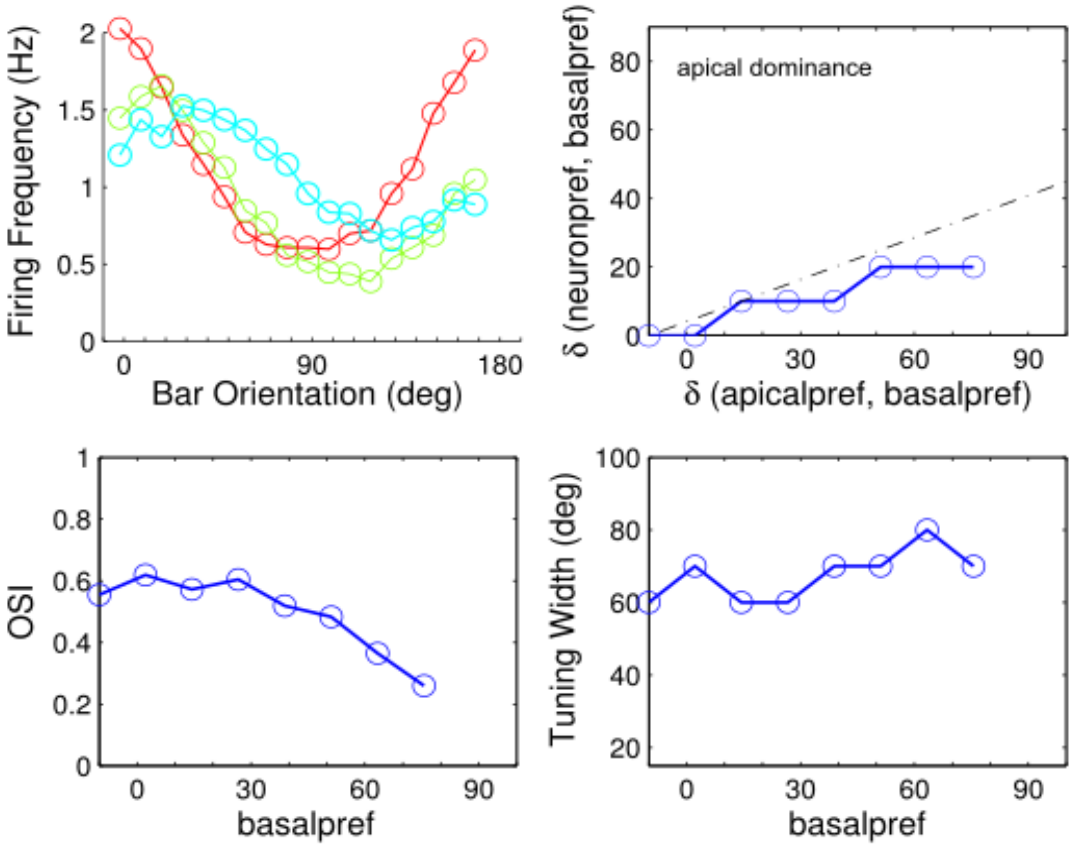

FIGURE 3.3. Orientation tuning curves when orientation preference in the apical and basal dendrites is the same ($\Delta = 0^o$, red tuning curve) or have 30^o or 60^o difference (cyan and green tuning curves respectively), preferred orientation, change in OSI and tuning width for different orientation preferences between the two trees.

3.4 Na+ & NMDA contribution

To assess the possible contribution of biophysical mechanisms, we simulate the blockade of voltage-gated Na^+ channels and/or NMDARs in basal and/or apical dendrites and measure the somatic firing rate in order to construct the corresponding tuning curves. In all cases the preferred orientation of the neuron was set to 0^o and the experiment consisted of 50 runs.

In addition, in each case we performed the same experiment with an increase of the AMPA conductance under NMDAR and/or Na^+ blockade, to account for the loss of excitability, so that the mean firing frequency in the non- preferred orientation is the same as in the control case and observed the differences with the control tuning curve.

3.4.1 Na+ blockade

Grading bars whose orientation varied from 0^o to 180^o with a step of 10^o were presented while g_{na} was set to 0 in the basal and the apical tree alternately. The somatic firing rate was measured for each step to construct the tuning curve for each case.

As seen in fig. 3.4, the blockade of dendritic voltage-gated Na+ channels has a larger effect on the firing frequency of the neuron when it is performed in the apical rather than the basal tree. However, when the AMPA conductance is increased by 10% it seems that the basal Na^+ has a larger contribution in the firing rate at the preferred orientation.

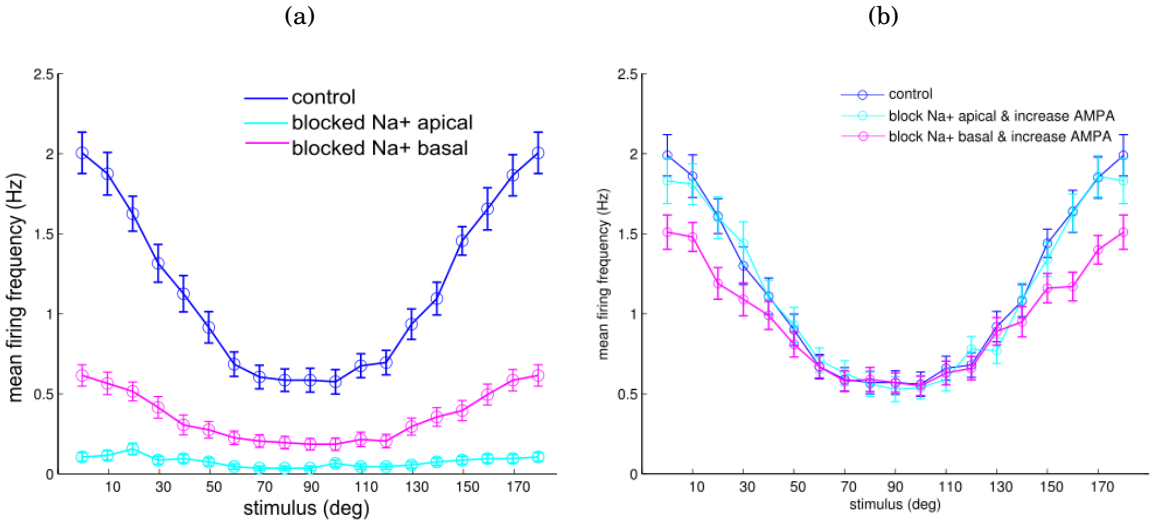

FIGURE 3.4. (a) blocked Na^+ tuning curves (b) blocked Na^+ plus increased AMPA conductance tuning curves.

3.4.2 NMDAR blockade

The same procedure was followed, but this time the conductance of the NMDARs was set to 0 first in the basal tree and then in the apical tree. As seen in fig. 3.5, NMDAR blockade influences tuning more when applied to the basal rather than the apical tree, though the observable difference is rather small. Increase of the AMPA conductance under NMDAR blockade by 10% amplified this difference and revealed that it is the basal NMDARs that enhance the orientation selectivity of the neuron and this is achieved by increasing its firing in the preferred orientation.

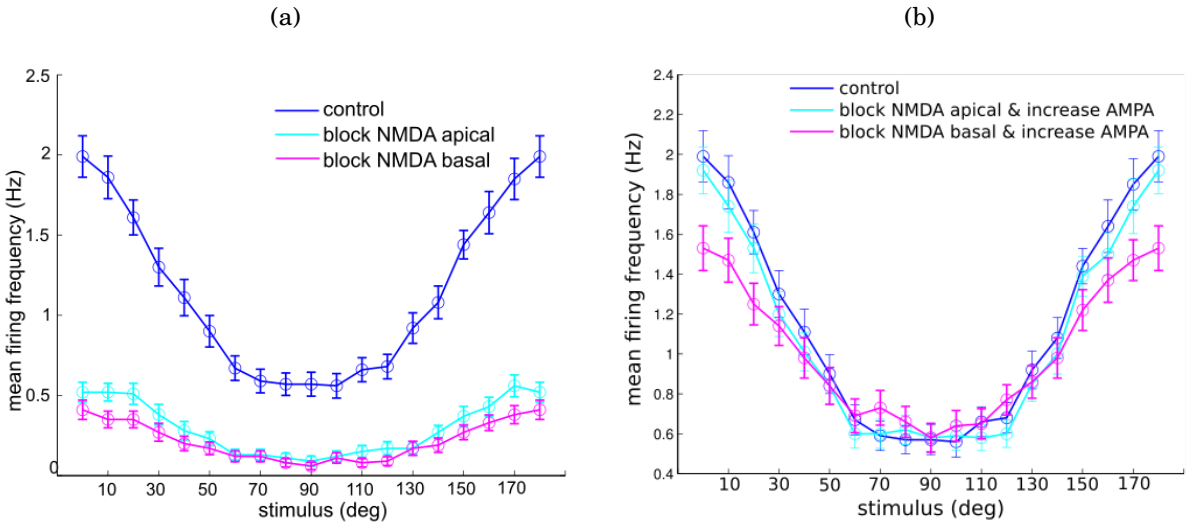

FIGURE 3.5. (a) blocked NMDARs tuning curves (b) blocked NMDARs plus increased AMPA conductance tuning curves.

3.4.3 Combined blockade

To acquire a more complete picture we performed the same procedure as above, but this time we blocked both the voltage-gated Na^+ channels and the NMDARs at the same time in the dendritic trees of the cell alternately to see the effect of the combined blockade. As expected, the combined blockade reduced so much the firing rate that we didn't have any tuning in either tree blockade. On the other hand, the tuning curves in the case of increased AMPA conductance by 20% for the basal and 25% for the apical blockade show that combined blockade of the basal tree has a larger effect than the apical tree.

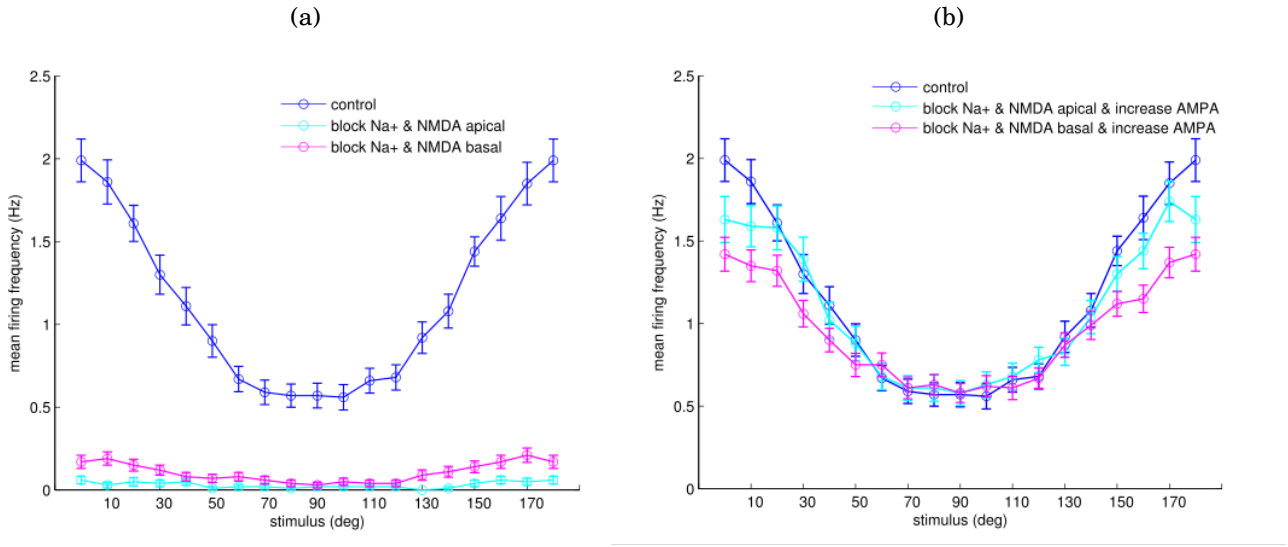

FIGURE 3.6. (a) blocked Na^+ and NMDARs tuning curves (b) blocked Na^+ and NMDARs plus increased AMPA conductance tuning curves.

Our data so far suggest a dominant role of the basal rather than the apical tree in fine tuning the orientation preference of these cells.

3.5 Dendritic events

In this section we record from the neuron's dendrites to search for regenerative dendritic events that may account for the results we acquired in the previous section. Again, the neuron's preferred orientation is set to 0^o and the experiment is repeated for 10 runs.

3.5.1 Na+ spikes

3.5.1.1 detection of dendritic spikes

Observing the voltage traces of the dendritic recordings one can easily notice the spikes. (fig. 3.7)

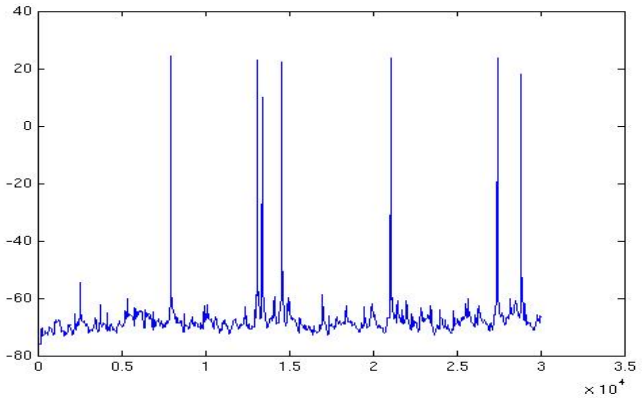

FIGURE 3.7. Exemplar dendritic trace.

Next, we examined if there is a difference in the number of Na spikes between the preferred and orthogonal orientation in the control case. Counting the number of dendritic Na spikes in each dendrite in the preferred and the orthogonal orientation, one can see in table 3.2 that almost 63% of the number of dendritic Na spikes is lost in the orthogonal orientation in the control case. The spike threshold was set at -40mV.

3.5.1.2 Na+ blockade

Subsequently, we recorded from the dendrites while we had blocked the voltage-gated Na+ channels in the apical and the basal tree separately. Blockade of the apical voltage-gated Na+ channels led to extinction of the Na+ spikes whereas blockade of the basal voltage-gated Na+ channels resulted in loss of amplitude, but not extinction of the spikes. So, our data suggest that apical dendrites can initiate Na^+ spikes on their own, which are boosted by the basal tree, whereas the basal dendrites are not capable of initiating Na^+ spikes on their own without facilitation from the apical tree. These results are in accordance with the tuning curves shown in fig. 3.4.

dendrite	0^o	90^o	%loss	dendrite	0^o	90^o	%loss
b1	11.3	5.5	51.32743363	a19	4.1	1.4	65.85365854
b2	4.1	1.4	65.85365854	a20	4.1	1.4	65.85365854
b3	4.1	1.4	65.85365854	a21	4.1	1.4	65.85365854
b4	4.1	1.4	65.85365854	a22	4.1	1.4	65.85365854
b5	4.1	1.4	65.85365854	a23	4.1	1.4	65.85365854
b6	4.1	1.4	65.85365854	a24	4.3	1.4	67.44186047
b7	4.1	1.4	65.85365854	a25	4.1	1.4	65.85365854
a1	4.1	1.4	65.85365854	a26	4.1	1.4	65.85365854
a2	4.1	1.4	65.85365854	a27	4.1	1.4	65.85365854
a3	4.1	1.4	65.85365854	a28	4.1	1.4	65.85365854
a4	4.1	1.4	65.85365854	a29	4.1	1.4	65.85365854
a5	4.1	1.4	65.85365854	a30	4.4	1.4	68.18181818
a6	4.1	1.4	65.85365854	a31	4.6	1.5	67.39130435
a7	4.1	1.4	65.85365854	a32	4.4	1.5	65.90909091
a8	4.1	1.4	65.85365854	a33	4.4	1.5	65.90909091
a9	4.1	1.4	65.85365854	a34	4.4	1.5	65.90909091
a10	4.1	1.4	65.85365854	a35	5.7	2.3	59.64912281
a11	6.4	3	53.125	a36	4.1	1.4	65.85365854
a12	6.4	3.1	51.5625	a37	4.1	1.4	65.85365854
a13	6	2.9	51.66666667	a38	4.1	1.4	65.85365854
a14	5.4	2.9	46.2962963	a39	4.1	1.4	65.85365854
a15	7	3.6	48.57142857	a40	4.3	1.4	67.44186047
a16	5.8	2.9	50	a41	4.3	1.4	67.44186047
a17	5.3	2.8	47.16981132	a42	4.3	1.4	67.44186047
a18	4.1	1.4	65.85365854	average loss	63.31360697	±6.12006194	-

Table 3.2: Dendritic firing frequency in the preferred and in the orthogonal orientation.

3.5.1.3 sensitivity analysis

In order to test whether the basal dendrites can support the initiation of Na+ spikes on their own we performed a sensitivity analysis, i.e. we increased gna in the basal dendrites so that they produce spikes and/or have an effect on the somatic firing.
As seen in fig. 3.8, by 15% increase in the g_{na} in the basal dendrites, only 2 dendrites spike, primarily because of basal 1, which is a long and thin branch, so is highly excitable. Increasing g_{na} in the basal dendrites by 30% induces dendritic spikes in many basal dendrites, but the somatic firing rate then is higher than the firing rate found in bibliography.
We should note that this analysis should be extended in order to try combinations of

increase in g_{na} in basal and decrease in g_{na} in the apical tree, so that the somatic firing frequency remains the same.

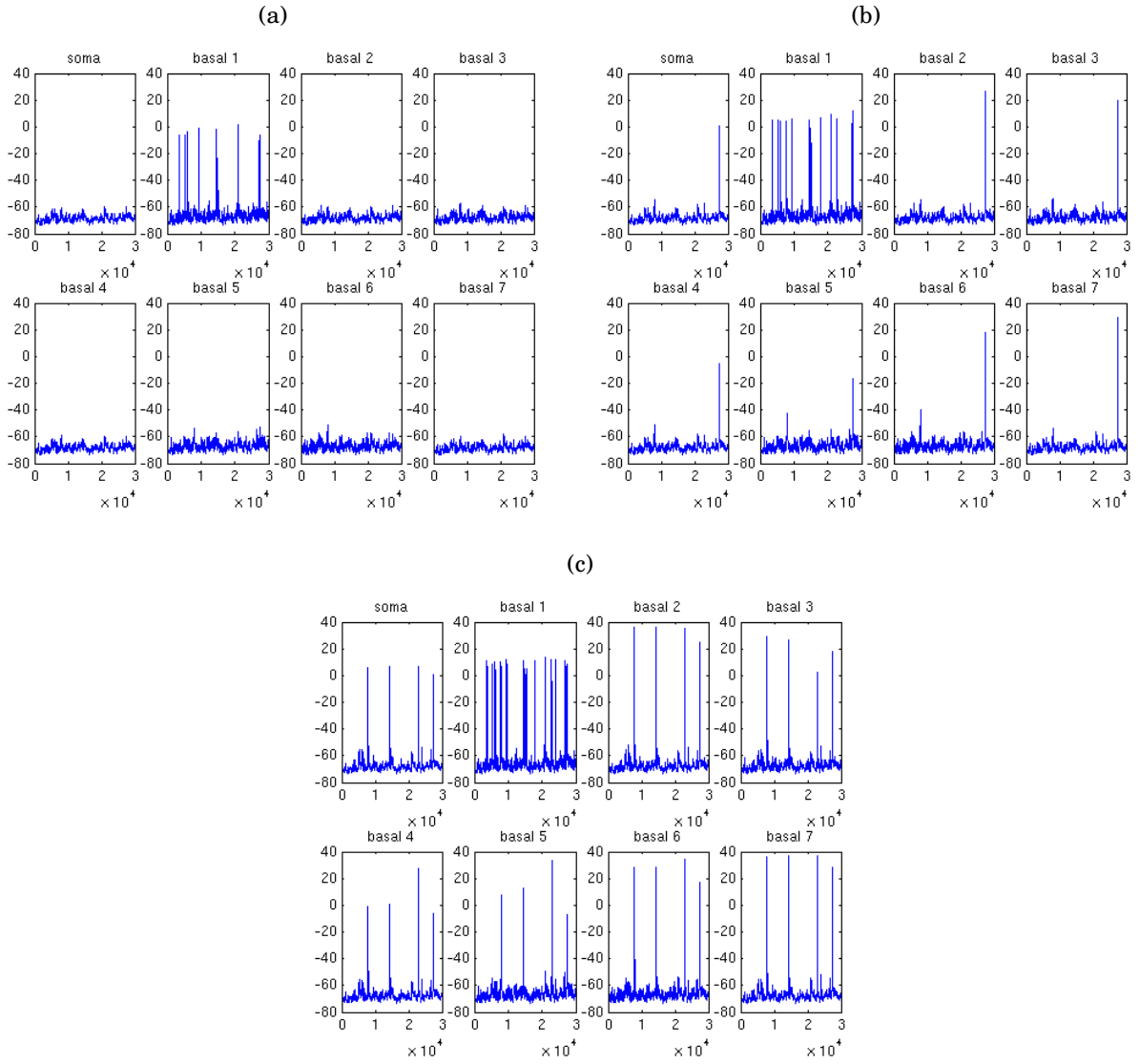

FIGURE 3.8. somatic and basal dendritic traces in the case of blocked na in the soma and the apical tree and for different g_{na} (a) control (b) basal g_{na} increased by 15% (c) basal g_{na} increased by 30%

3.5.1.4 Na+ spikes timing

To continue the study of the contribution of dendritic Na+ spikes we compared dendritic spike timing to the somatic timing for each dendrite in the control case and based on that we divided the dendritic spikes in 4 categories:

* back-propagating, i.e.spikes that initiated in the soma or in an other dendrite and propagated back to the dendrite

* forward-propagating, i.e.spikes that initiated in the dendrite and then propagated to the soma

* identical, i.e. spikes that had the same timing or a difference of 0.1ms

* spikes that were created in the dendrite, but did not make it to the soma

The number of spikes of each category is shown in table 3.3 where it is clear that there is a statistically important decrease in all categories (p_1=0.0001, p_2=0.006, p_3=0.0004, p_4=0.0003). The percentages of each category, i.e. the number of spikes of each category to the total number of the dendritic spikes, were calculated and we wanted to see whether these percentages differ and in what way between the preferred orientation and the orthogonal one. Though there seems to be a decrease in the percentage of back-propagating dendritic spikes and in the identical ones and an increase in the forward-propagating spikes and in those that didn't make it to the soma, the only statistically important difference is the increase in the percentage of the forward-propagating dendritic spikes (p_1=0.028, p_2=0.135, p_3=0.095, p_4=0.078). The results are shown in figure 3.10.

	run	1	2	3	4	5	6	7	8	9	10
pref	back	126	80	63	110	53	55	137	67	49	135
	forward	43	42	62	42	16	35	89	55	22	37
	identical	76	74	71	92	29	57	117	74	27	73
	didnt make it	31	29	42	32	25	29	50	51	32	32
	total	276	225	238	276	123	176	393	247	130	277
ortho	back	51	11	31	13	16	0	36	12	11	58
	forward	37	20	35	18	15	0	11	18	21	53
	identical	57	18	32	18	15	0	11	18	21	33
	didnt make it	19	19	25	20	14	11	12	23	20	33
	total	164	68	123	69	63	11	61	72	69	180

Table 3.3: Number of spikes for each category in the preferred and in the orthogonal orientation

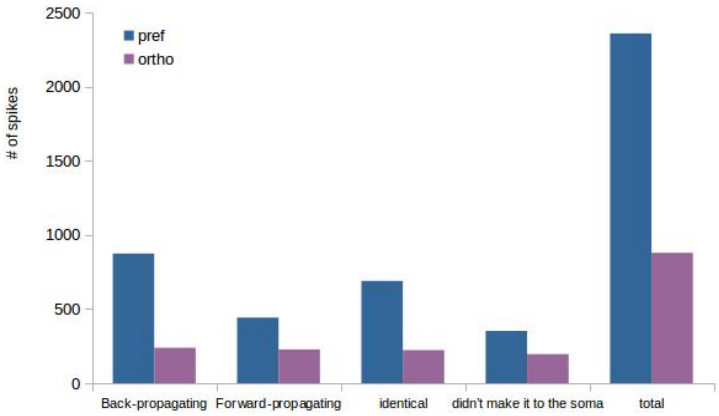

FIGURE 3.9. Number of spikes for each category.

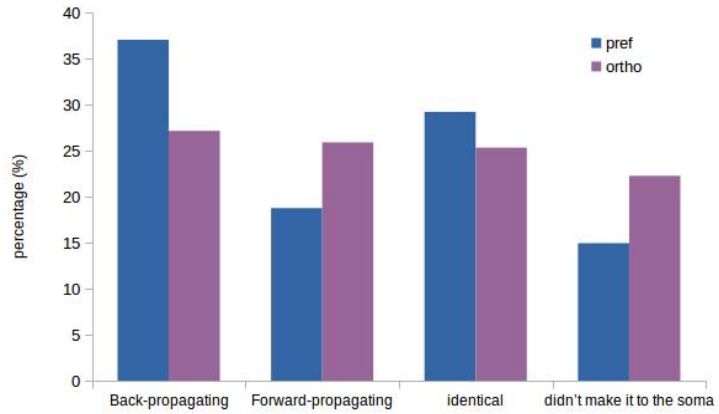

FIGURE 3.10. Comparison of percentages in the preferred and the orthogonal orientation.

The next question to answer is what percentage of the somatic spikes is caused by the dendrites.

	soma	dendrite	
		apical	basal
pref	4	17	10
ortho	-	11	3

Table 3.4: Origin of somatic spikes

In the preferred orientation 41.46% of the somatic spikes is of apical origin, 24.39% is of basal origin and 9.76% is of somatic origin. In the orthogonal orientation there are

no spikes of somatic origin, whereas 78.57% is originated in the apical dendrites and 21.42% in the basal.

3.5.2 NMDA contribution

3.5.2.1 detection of dendritic spikes

Next, we tried to see if there are NMDA spikes in our model. The methodology was as follows:

* block voltage-gated Na^+ channels in the whole cell and record from each dendrite
* also block NMDARs in both dendritic trees and record from the dendrites
* substract the second trace from the first (block Na^+ everywhere-(block Na^+ everywhere+block NMDA))
* search for outliers, i.e. values of more than 3*std above mean (fig. 3.12)

In table 3.5 is the total duration and the number of outlying assembles found in basal and apical dendrites in both the preferred and the orthogonal orientation. The amplitude of these 'spikelets' is of the order of 2-3mV, so they cannot acount for NMDA spikes. Moreover, as we can see in table 3.5, there is no significant difference between the preferred and the orthogonal orientation.

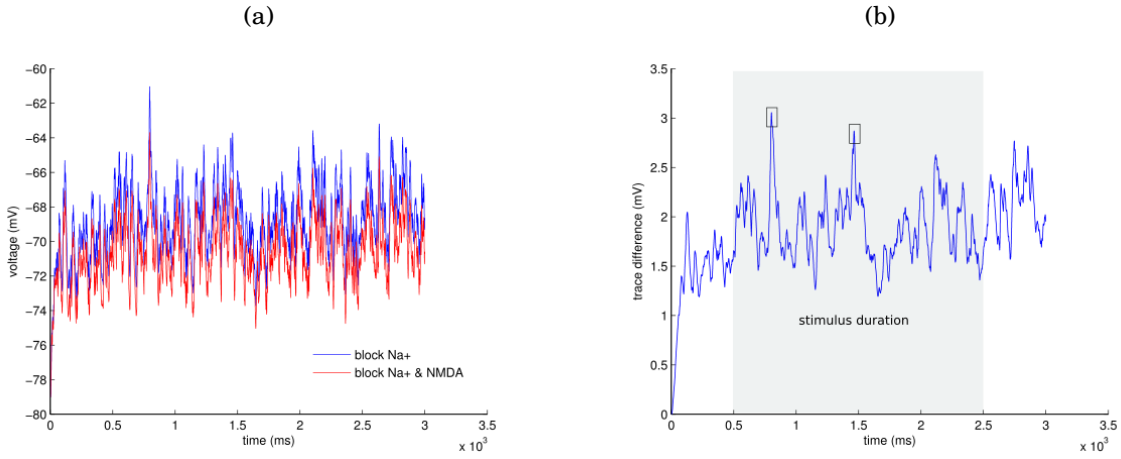

FIGURE 3.11. (a) traces with blocked Na^+ everywhere and blocked Na^+ everywhere plus blocked NMDARs (b) difference of these traces

	basal		apical		total	
	#	total dur (ms)	#	total dur (ms)	#	total dur (ms)
pref	53	559.5	253	2757.1	306	3316.6
ortho	47	500.1	350	3046.1	397	3546.1

Table 3.5: Number and duration of outlying values

CHAPTER 4

DISCUSSION

To make sense of the world around us and the constant flow of environmental stimuli that it receives the brain has developed a quite efficient way: feature selectivity. This refers to the property of certain neuronal populations to respond more vigorously to specific stimuli, e.g. a specific tone frequency and weakly to the others. Feature selectivity is a fundamental property of sensory processing, which is used by the visual (Hubel & Wiesel 1959), the auditory (Goldstein et al. 1970), the tactile (Lichtenstein et al. 1990) and the olfactory system (Yoshida & Mori, 2007), but is mostly studied in the visual system. The story began in the 50's with the work of Hubel and Wiesel, who discovered what may be the most studied case of feature selectivity: orientation preference (Hubel & Wiesel 1959,1968).

However, there is still a lot that remains unanswered and needs to be explained, particularly in the single cell and dendritic level where the technological limitations that existed until recently have slowed things down. Recent studies though, using state of the art technologies have started to provide us with useful information regarding orientation selectivity from the circuit to the dendritic level (Ko et al. 2011, Ko et al.2011, Jia et al. 2010. Chen et al. 2013).

Layer 2/3 pyramidal neurons, with their complex morphological and biophysical architecture are cells that can support dendritic spikes (Larkum 2007), which can affect the neuron's firing by increasing the propability for a somatic action potential and/or by interacting with back-propagating action potentials. Sensory-evoked dendritic spikes have been detected in several sensory cortices: visual (Smith et al. 2013), auditory (Chen

et al. 2011), somatosensory (Palmer et al. 2014) and barrel cortex (Lavzin et al. 2012).

What is more, pyramidal neurons have two distinct morphological compartments, i.e. the basal and apical tree, where the basal tree receives mainly feed-forward input, whereas the apical tree receives intracortical feedback input. This fact could possibly mean that these two trees have different importance or contribution to the emergence of orientation selectivity in the single cell level and even act as an association of the external environment with our internal representation (Larkum 2013).

In this study we tried to study the feature of orientation selectivity that layer 2/3 pyramidal neurons exhibit in the dendritic level on the primary visual cortex of the mouse. Moreover we examine the possibility for the basal and apical trees to have dinstict roles in the emergence of the particular feature.

The results of the first part of the study show that orientation tuning of the neuron seems to follow the tuning of the basal tree. Blockade of dendritic voltage-gated Na^+ channels has a larger effect on the firing frequency of the neuron when it is performed in the apical rather than the basal tree, in which case tuning is completely lost. However, when the AMPA conductance is increased it is the basal tree that has the biggest influence. NMDAR blockade influences tuning primarily when applied to the basal rather than the apical tree. Increase of the AMPA conductance to account for the loss of excitability under NMDAR blockade, reveals that it is the basal NMDARs that enhance the orientation selectivity of the neuron and this is achieved by increasing its firing in the preferred orientation, whereas apical NMDA currents dont́ seem to have a significant contribution in the cellś tuning. Overall, these results attribute to the basal tree a more significant role in shaping orientation selectivity in layer 2/3 V1 pyramidal neurons.

When we moved to the dendritic level, we found that the neuron produces Na^+ spikes and the number of these spikes is significantly larger in the preferred orientation than in the orthogonal one. Regarding the fact that our data show that the basal dendrites are not capable of initiating Na^+ spikes on their own, but only with the help of the apical tree, a more exhaustive sensitivity analysis, including manipulation of the g_{na} in both trees, is needed in order to find a condition in which it is feasible to have Na^+ spikes of exclusively basal origin. This condition is perhaps more intuitionally correct, but there are no experimental data on the sodium conductance in each tree or showing that basal dendrites can independently produce dendritic spikes. For this reason, we keep the existing configuration which is agreement with data from the Smirnaki's lab.

Regarding our search for possible existence of NMDA spikes, we failed to find any. We only indicated some spikelets, which were of small amplitude (2-3mV) and duration

(1ms-30ms) and did not differ between preferred and orthogonal orientations. What should be done further in this part of the study is to involve also the potassium channels, which are known to play a role in NMDA spikes (Bock & Stuart, 2016) and also perfom the analysis in the case of increased AMPA conductance. Previous studies (Smith et al. 2013) have shown that there is an NMDA component enhancing, not producing, orientation selectivity.

There are also certain limitations in our study. These include the fact we did not take into consideration the role of inhibition in orientation selectivity. It has been shown, for instance, that inhibitory interneurons sharpen the already existing orientation selectivity by lowering the membrane potential for all orientations, but mostly for the orthogonal orientation. In addition, we did not take into account connectivity in the circuit level, where it has been shown that few strong connected pairs with similar orientation account for the majority of the total synaptic weight. Moreover, the model was based on experiments on anaesthetised animals, which constitutes another restriction to our work.

So, in the future the model should be adjusted to overcome the aforementioned limitations. Moreover, more morphologies should be acquired and modeled in order to have a more complete picture.

APPENDIX A

Useful definitions

orientation selectivity: the stronger response of the neuron to a certain orientation compared to the others
firing rate: the number of spikes divided by the duration of the stimulus presentation in seconds
preferred / orthogonal orientation: the preferred orientation is the one that neuron responds the strongest, whereas the orthogonal is the orientation the neuron responds weak and is perpendicular to the preferred one.
tuning curve: diagram that consists of the firing frequency of the cell in each orientation

BIBLIOGRAPHY

Arenkiel, B. R., Peca, J., Davison, I. G., Feliciano, C., Deisseroth, K., Augustine, G. J., ... & Feng, G. (2007). In vivo light-induced activation of neural circuitry in transgenic mice expressing channelrhodopsin-2. Neuron, 54(2), 205-218.

Bock, T., & Stuart, G. J. (2016). Impact of calcium-activated potassium channels on NMDA spikes in cortical layer 5 pyramidal neurons. Journal of neurophysiology, 115(3), 1740-1748.

Bock, D. D., Lee, W. C. A., Kerlin, A. M., Andermann, M. L., Hood, G., Wetzel, A. W., ... & Reid, R. C. (2011). Network anatomy and in vivo physiology of visual cortical neurons. Nature, 471(7337), 177-182.

Carnevale, N.T. and Hines, M.L. The NEURON Book. Cambridge, UK: Cambridge University Press, 2006.

Caze, R., Jarvis, S. & Schultz, S. (2015) Non-linear dendrites enable robust stimulus selectivity. bioRxiv

Chen, T. W., Wardill, T. J., Sun, Y., Pulver, S. R., Renninger, S. L., Baohan, A., ... & Looger, L. L. (2013). Ultrasensitive fluorescent proteins for imaging neuronal activity. Nature, 499(7458), 295-300.

Chen, X., Leischner, U., Rochefort, N. L., Nelken, I., & Konnerth, A. (2011). Functional mapping of single spines in cortical neurons in vivo. Nature,475(7357), 501-505.

Cho, K. H., Jang, J. H., Jang, H. J., Kim, M. J., Yoon, S. H., Fukuda, T., ... Rhie, D. J. (2010). Subtype-specific dendritic Ca2+ dynamics of inhibitory interneurons in the rat

visual cortex. Journal of neurophysiology, 104(2), 840-853.

Colbert, C. M., Magee, J. C., Hoffman, D. A., & Johnston, D. (1997). Slow recovery from inactivation of Na+ channels underlies the activity-dependent attenuation of dendritic action potentials in hippocampal CA1 pyramidal neurons. The Journal of neuroscience, 17(17), 6512-6521.

Cossell, L., Iacaruso, M. F., Muir, D. R., Houlton, R., Sader, E. N., Ko, H., ...& Mrsic-Flogel, T. D. (2015). Functional organization of excitatory synaptic strength in primary visual cortex. Nature.

Cruz-Martin, A., El-Danaf, R. N., Osakada, F., Sriram, B., Dhande, O. S., Nguyen, P. L., ... Huberman, A. D. (2014). A dedicated circuit links direction-selective retinal ganglion cells to the primary visual cortex. Nature, 507(7492), 358-361.

DeFelipe, J., Farinas, I. (1992). The pyramidal neuron of the cerebral cortex: morphological and chemical characteristics of the synaptic inputs. Progress in neurobiology, 39(6), 563-607.

Drager, U. C. (1978). Observations on monocular deprivation in mice. J. Neurophysiol. 41, 28,Äì42

Goldstein, Jr, M., Abeles, M., Daly, R. L., and McIntosh, J. (1970). Functional architecture in cat primary auditory cortex: tonotopic organization. J Neurophysiol, 33(1):188,Äì197.

Hofer, S. B., Ko, H., Pichler, B., Vogelstein, J., Ros, H., Zeng, H., ... & Mrsic-Flogel, T. D. (2011). Differential connectivity and response dynamics of excitatory and inhibitory neurons in visual cortex. Nature neuroscience, 14(8), 1045-1052.0

Hubel, D. H., Wiesel, T. N. (1959). Receptive fields of single neurones in the cat's striate cortex. The Journal of physiology, 148(3), 574-591.

Hubel, D. H. and Wiesel, T. N. (1968). Receptive fields and functional architecture of monkey striate cortex. J Physiol, 195(1):215,Äì243.

Hubener, M. (2003). Mouse visual cortex. Current opinion in neurobiology, 13(4), 413-420.

Hudspeth, A. J., Logothetis, N. K. (2000). Sensory systems. Current opinion in neurobiology, 10(5), 631-641.

Jaffe, D. B., Johnston, D., Lasser-Ross, N., Lisman, J. E., Miyakawa, H., & Ross, W. N. (1992). The spread of Na+ spikes determines the pattern of dendritic Ca2+ entry into hippocampal neurons. Nature, 357(6375), 244-246.

Jeon, C.J., Strettoi, E., Masland, R.H. (1998) The major cell populations of the mouse retina. J Neurosci. 18, 8936-8946.

Jia, H., Rochefort, N. L., Chen, X., & Konnerth, A. (2010). Dendritic organization of sensory input to cortical neurons in vivo. Nature, 464(7293), 1307-1312

Ko, H., Hofer, S. B., Pichler, B., Buchanan, K. A., Sjostrom, P. J., & Mrsic-Flogel, T. D. (2011). Functional specificity of local synaptic connections in neocortical networks. Nature, 473(7345), 87-91.

Ko, H., Cossell, L., Baragli, C., Antolik, J., Clopath, C., Hofer, S. B., & Mrsic-Flogel, T. D. (2013). The emergence of functional microcircuits in visual cortex. Nature, 496(7443), 96-100.

Koch, C., Poggio, T., & Torre, V. (1983). Nonlinear interactions in a dendritic tree: localization, timing, and role in information processing. Proceedings of the National Academy of Sciences, 80(9), 2799-2802.

Larkum, M. E., Waters, J., Sakmann, B., & Helmchen, F. (2007). Dendritic spikes in apical dendrites of neocortical layer 2/3 pyramidal neurons. The Journal of Neuroscience, 27(34), 8999-9008.

Larkum, M. (2013). A cellular mechanism for cortical associations: an organizing principle for the cerebral cortex. Trends in neurosciences, 36(3), 141-151.

Lavzin, M., Rapoport, S., Polsky, A., Garion, L., & Schiller, J. (2012). Nonlinear dendritic processing determines angular tuning of barrel cortex neurons in vivo. Nature, 490(7420), 397-401.

Li, Y. T., Ibrahim, L. A., Liu, B. H., Zhang, L. I., & Tao, H. W. (2013). Linear transformation of thalamocortical input by intracortical excitation. Nature neuroscience, 16(9), 1324-1330.

Lichtenstein, S. H., Carvell, G. E., & Simons, D. J. (1990). Responses of rat trigeminal ganglion neurons to movements of vibrissae in different directions. Somatosensory & motor research, 7(1), 47-65.

Lien, A. D., & Scanziani, M. (2013). Tuned thalamic excitation is amplified by visual cortical circuits. Nature neuroscience, 16(9), 1315-1323.

Liu, B. H., Li, Y. T., Ma, W. P., Pan, C. J., Zhang, L. I., & Tao, H. W. (2011). Broad inhibition sharpens orientation selectivity by expanding input dynamic range in mouse simple cells. Neuron, 71(3), 542-554.

Longordo, F., To, M. S., Ikeda, K., & Stuart, G. J. (2013). Sublinear integration underlies binocular processing in primary visual cortex. Nature neuroscience,16(6), 714-723.

Luo, L., Callaway, E. M., & Svoboda, K. (2008). Genetic dissection of neural circuits. Neuron, 57(5), 634-660.

Niell, C. M., & Stryker, M. P. (2008). Highly selective receptive fields in mouse visual cortex. The Journal of Neuroscience, 28(30), 7520-7536.

Ohki, K., Chung, S., Ch'ng, Y.H., Kara, P. and Reid, R.C., 2005. Functional imaging with cellular resolution reveals precise micro-architecture in visual cortex. Nature, 433(7026), pp.597-603.

Palmer, L. M., Shai, A. S., Reeve, J. E., Anderson, H. L., Paulsen, O., & Larkum, M. E. (2014). NMDA spikes enhance action potential generation during sensory input. Nature

neuroscience, 17(3), 383-390.

Poirazi, P., & Mel, B. W. (1999). Towards the memory capacity of neurons with active dendrites. Neurocomputing, 26, 237-245.

Smith, S. L., Smith, I. T., Branco, T., & Hausser, M. (2013). Dendritic spikes enhance stimulus selectivity in cortical neurons in vivo. Nature, 503(7474), 115-120.

Stuart, G., Spruston, N., Sakmann, B., & Hausser, M. (1997). Action potential initiation and backpropagation in neurons of the mammalian CNS. Trends in neurosciences, 20(3), 125-131.

Stuart, G. J., & Spruston, N. (2015). Dendritic integration: 60 years of progress. Nature neuroscience, 18(12), 1713-1721.

Yoshida, I., & Mori, K. (2007). Odorant category profile selectivity of olfactory cortex neurons. The Journal of Neuroscience, 27(34), 9105-9114.

Vetter, P., Roth, A., & Hausser, M. (2001). Propagation of action potentials in dendrites depends on dendritic morphology. Journal of neurophysiology, 85(2), 926-937.

Zhao, X., Liu, M., & Cang, J. (2013). Sublinear binocular integration preserves orientation selectivity in mouse visual cortex. Nature communications, 4.